

Revealing vibronic coupling in chlorophyll *c1* by polarization-controlled 2D electronic spectroscopy

Eglė Bukartė¹, Anja Haufe², David Paleček³, Claudia Büchel², Donatas Zigmantas^{1*}

¹Chemical Physics, Lund University, Sweden

²Institute of Molecular Biosciences, Goethe University Frankfurt, Germany

³Cavendish Laboratory, University of Cambridge, United Kingdom

[*donatas.zigmantas@chemphys.lu.se](mailto:donatas.zigmantas@chemphys.lu.se)

Abstract

Vibronic coupling between molecules has been recently discussed to play an important role in photosynthetic functions. Furthermore, this type of coupling between electronic states has been suggested to define photophysical properties of chlorophylls, a family of photosynthetic molecules. However, experimental investigation of vibronic coupling presents a major challenge. One subtle way to study this coupling is by excitation and observation of the superpositions of vibrational states via transitions to vibronically mixed states. Such superpositions, called coherences, are then observed as quantum beats in non-linear spectroscopy experiments. Here we present polarization-controlled two-dimensional electronic spectroscopy study of the chlorophyll *c1* molecule at cryogenic (77 K) temperature. By applying complex analysis to the oscillatory signals we are able to unravel vibronic coupling in this molecule. The vibronic mixing picture that we see is much more complex than was thought before.

Keywords

Vibronic coupling, two-dimensional electronic spectroscopy, photosynthetic pigments, chlorophyll c1, polarization-controlled multidimensional spectroscopy.

Introduction

Chlorophylls and chlorophyll-like molecules have received a significant amount of attention through the years due to their major role in photosynthesis, as they belong to the main molecular group responsible for light absorption, excitation energy transfer and charge separation during the solar energy utilization process[1]. Naturally, a lot of effort has been dedicated to trying to understand the electronic structure and excitation dynamics of these molecules. The well-known Gouterman model, originally applied to the porphyrin molecules, describes two main transitions in chlorophylls as separate electronic transitions, denoted as Q_y and Q_x , with almost perpendicular mutual orientation of transition dipole moments[2]. However, a recent comprehensive study of a wide range of chlorophyll-like molecules has shown that vibronic coupling between these two states must be taken into account in order to describe the photophysical properties and excitation dynamics in these molecules correctly[3].

Here we use a definition of the vibronic coupling as follows: it is an interaction between the purely electronic transition to the higher energy state (Q_x) and vibronic transition of the lower energy state ($Q_y +$ a vibrational quantum $\tilde{\nu}$). This vibronic coupling entails sharing of the oscillator strength between the states, as well as mixing of their characters, resulting in reorientation of the transition dipole moments[3,4]. The mixing of the states depends both on coupling strength and resonance detuning between Q_x and $Q_y + \tilde{\nu}$ transitions. It is noteworthy, that vibronic coupling in molecular dimers and bigger aggregates was suggested to speed up energy transfer in multichromophore complexes[4,5]. Although the presence of vibronic coupling in chlorophylls is anticipated, it is very difficult to observe it experimentally, which is the aim of this study.

Two-dimensional electronic spectroscopy (2DES) is a very well-suited technique to explore couplings and superpositions between quantum states[6,7]. Specifically, it has been employed for studying vibrational coherences in chlorophyll-type molecules[8–10]. However, to observe the vibronic coupling between two electronic energy states is challenging. There are several technical complications involved, since energy splitting between the tentative Q_y and Q_x transitions is large, it is difficult to excite their superposition with the same laser pulse[3]. Additionally, the Q_x transition (higher in energy) is generally very weak and 2D signals scale super-linearly with the transition dipole moment. Therefore, high dynamic range of detection is required to discern signals arising from the coupling between the two states[11]. Lastly, the most common 2DES experiments are done with the polarization of all laser pulses set parallel to each other. Such experiments have no selectivity for detecting vibronically coupled transitions, and instead they are dominated by the Franck-Condon vibrational wavepacket signals on the ground and excited electronic states.

To explore the vibronic coupling between the Q_y and Q_x states in chlorophyll molecules we performed polarization-controlled 2DES at 77 K on chlorophyll (Chl) *c1* molecules, extracted from the diatom *Cyclotella meneghiniana*, where they are found in light-harvesting complexes. In contrast to most chlorophylls, which are chlorins, Chl *c* is a porphyrin with an acrylic acid side chain (see [12] and Fig. S1). Our choice of the Chl *c1* is based on the fact that it features two lowest absorption bands (tentatively denoted as Q_y and Q_x and we will use this notation in the following) having similar intensity. Close position in energy also makes it feasible to cover them both with a laser spectrum (Fig. 1). Due to these favorable properties, we expect vibronic coupling to be detectable. Two sets of 2DES experiments were performed: a standard all-parallel arrangement, with all four laser pulses having the same linear polarization with respect to each other ($(0^\circ, 0^\circ, 0^\circ, 0^\circ)$, AP), and a double-crossed polarization sequence, where polarization of the pulse pairs have the offset of 90° with respect to each other ($(45^\circ, -45^\circ, 90^\circ, 0^\circ)$, DC). The major advantage of the DC polarization sequence is that it is specifically sensitive to detecting vibronic coupling in molecular systems[13–15].

Materials and Methods

Sample preparation

Chl *c1* (structure shown in Fig. S1 in Supplementary Information (SI)) was isolated from the diatom *Cyclotella meneghiniana* (Culture Collection Göttingen, strain 1020-1a) that had been

cultured for 7 days at 18°C in modified ASP medium according to [16] under 40 $\mu\text{mol quanta m}^{-2} \text{s}^{-1}$ of white light, with 16 h light and 8 h dark constant shaking at 120 rpm.

Cells were harvested by centrifugation at 4304 g for 15 min at 4°C and homogenized in liquid nitrogen using pestle and mortar. All steps were carried out in almost complete darkness. After adding a small amount of CaCO_3 , 80 ml Acetone, 8 ml concentrated NaCl solution and 80 ml diethyl ether were added. In a separating funnel, phase separation was improved by adding drops of water. The upper phase was evaporated in a rotary evaporator after the remaining water had been removed by Sephadex G25. The pigments were resolved in acetone, and Chl *a* and Chl *c1* concentration determined according to [17].

Sample equivalent to 1 mg Chl *a* was loaded on a column of microcrystalline cellulose equilibrated with petrol ether (50-70°C). The column was washed with petrol ether (50-70°C) until Chl *a* eluted. After washing with 300 mL 2% n-propanol in petrol ether (50-70°C), Chl *c1* was eluted using 20 ml of 25% methanol in diethyl ether. At this stage some contamination with fucoxanthin was still present, thus pigments were again dried in a rotary evaporator, solved with petrol ether (50-70°C) and loaded on a new column of the same material as described above. The column was washed with about 20-30 mL 5% methanol in diethylether until fucoxanthin was eluted, afterwards Chl *c1* was eluted with 20 ml 20-30 mL 25% methanol in diethylether. Quality was assessed by taking absorption spectra [18]. The solution was dried under N_2 and stored at 4°C in darkness until use.

For 2DES experiments, the sample was dissolved in isopropanol. The concentration corresponded to OD of 0.15 for the Q_y transition in the 0.2 mm optical path cuvette at 77 K (see Fig. 1 for the low temperature absorption spectrum).

Multidimensional spectroscopy experiments

2DES experiments have been described in details elsewhere [19,20]. In short, a lab-built non-collinear optical amplifier (NOPA) was pumped with a Pharos laser system (Light Conversion), pulse-picked at 2 kHz repetition rate, to produce laser pulses with ~ 100 nm FWHM bandwidth, centered at 600 nm. The pulses at the sample spot were compressed to 12 fs, using a pair of chirped mirrors and a prism compressor. The NOPA pulse was first split into two using a plate beamsplitter and both pulses were transmitted through a transmission grating beamsplitter to create two pairs of identical phase-locked pulses. In order to have full control of polarizations during the experiments, each pulse was transmitted first through a broadband quarter wave plate (to achieve the circular polarization) and then through an adjustable linear polarizer. In addition, another linear polarizer was placed in the detection pathway to filter out specific signal polarization.

Experimental conditions for both AP and DC experiments were kept as similar as possible. Excitation energy was ~ 6 nJ per pulse and all pulses were focused to a ~ 160 μm spot size. Population time was scanned in 10 fs time steps from 0 to 1670 fs in the AP experiment and from 0 to 1330 fs in the DC experiment. Early population times (0–80 fs for AP and 0–40 fs for DC) were omitted from the analysis due to the pulse overlap artifacts [21], which include non-resonant signals as well as scattering. Coherence time was scanned with movable fused silica wedges from -30 fs to 200 fs in steps of 1.5 fs in both experiments. After Fourier transformation, this corresponded to a resolution of 83 cm^{-1} on the excitation axis ($\tilde{\nu}_1$), whereas resolution on the

detection axis ($\tilde{\nu}_3$) was 52 cm^{-1} . All 2D spectra are shown after the interpolation to 200×200 data points.

Complex data analysis of oscillation signals

AP and DC data sets comprised of (45, 69) and (45, 61) data points along ($\tilde{\nu}_1, \tilde{\nu}_3$) respectively. Purely oscillating residuals were extracted by fitting and subtracting monotonically decaying signals, using independent 2-exponential fits for each point of the real and imaginary parts of the 2D spectrum. Time ranges of the fits and analyzed residuals were restricted to 80–1670 fs and 40–1330 fs for the AP and DC experiments, respectively. The oscillating signal residuals were interpolated to the 200×200 grid in the same way as the other 2D spectra presented in the main text. Complex FT for each ($\tilde{\nu}_1, \tilde{\nu}_3$) point along the population delay t_2 leads to the FT amplitude maps, so called oscillation maps, relating coherence wavenumber amplitude $\tilde{\nu}_2$ to the spectral position in the 2D spectrum ($\tilde{\nu}_1, \tilde{\nu}_3$) [22,23]. From the complex analysis, positive and negative $\tilde{\nu}_2$ oscillation maps were constructed, allowing us to separate beating signals in the ground and excited states [14,24]. No padding or apodization was used. The resulting $\tilde{\nu}_2$ wavenumber resolution was limited by the population delay scan range, and was $\sim 20 \text{ cm}^{-1}$ for AP and $\sim 25 \text{ cm}^{-1}$ for DC.

Results

Chlorophyll c1 absorption at cryogenic temperature

The low temperature (77 K) absorption spectrum of Chl *c1* is presented in Fig. 1 together with the laser spectrum used in the 2DES experiments. Absorbance was obtained by measuring the transmitted laser spectrum (intensity) in the 2DES setup with (I) and without (I_0) the sample and taking the common logarithm of the ratio of the two intensities (I_0/I). We note here that this type of absorption measurement is susceptible to the effect of the self-interference of the laser beam, which could result in a low amplitude periodic modulation of the absorption spectrum.

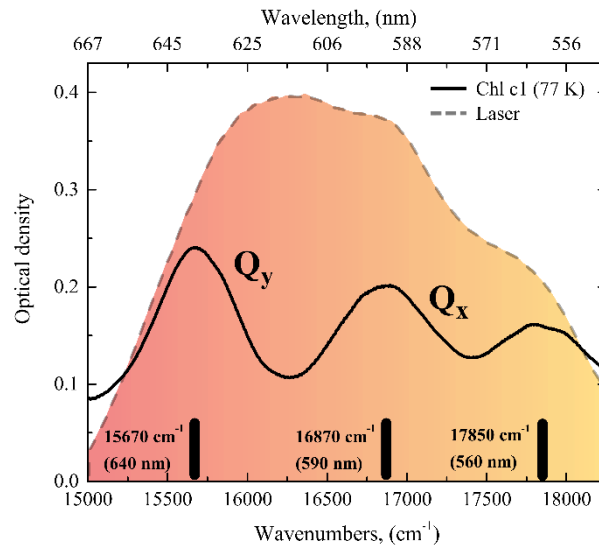


Fig. 1. Absorption spectrum of Chl *c1* at 77 K. Black solid line shows the absorption spectrum of Chl *c1* together with the laser spectrum (shaded) used in 2DES experiments. Center positions of three visible bands are marked with black solid bars. It can be clearly seen that transitions (marked Q_y and Q_x) have similar strength.

Solid vertical bars show the transitions visible at 77 K: Q_y at 15670 cm^{-1} and Q_x at 16870 cm^{-1} . In this work we employ the notation where Q_x lies higher in energy than Q_y , according to Helfrich et al.[12] Switching assignment of the two states would have no effect on the interpretation of the data presented below. The energy spacing between the two lowest transitions, evaluated from the low temperature absorption spectrum, is $\sim 1200\text{ cm}^{-1}$. The third transition, visible at 17850 cm^{-1} is most likely a higher-energy band arising from the coupling between the purely electronic Q_x and the vibronic transition $Q_y + \tilde{\nu}$ [3]. At room temperature, the higher energy peak is visible only as a weak shoulder (see [25] and Fig. S2 in SI). Since the third transition is located on the steep slope of the laser spectrum and therefore is excited rather weakly, it is not visible in the 2DES experiments (see Fig. 2 for 2DES AP spectrum).

Polarization-controlled 2DES

The real part of the total (rephrasing + non-rephasing) 2D spectra measured with the AP (left) and DC (right) polarization sequences at population time $t_2=100\text{ fs}$ are presented in Fig. 2. The AP spectrum features two diagonal peaks, corresponding to the Q_y and Q_x transitions. The weak negative signals above the positive peaks at detection wavenumber $\tilde{\nu}_3=16200\text{ cm}^{-1}$ correspond to excited state absorption to higher states.

The transition energies of the two electronic states, determined from the 2D spectra, are $\sim 15750\text{ cm}^{-1}$ and $\sim 16750\text{ cm}^{-1}$, resulting in the energy spacing of $\sim 1000\text{ cm}^{-1}$. The mismatch between the energies of transitions obtained from the AP 2D spectrum and from the low temperature absorption spectrum likely comes from the effect of a limited laser spectrum. Since it does not cover both transitions perfectly, it can cause a shift of the peaks in the 2D spectrum. Nevertheless, this does not influence analysis and conclusions presented in this work.

It is clear from the AP 2D spectrum measured at 100 fs that the relative intensities of the diagonal peaks are not the same as in the absorption profile. The major reason for this is a very fast internal relaxation between the Q_x and Q_y states, as discussed in detail below. Moreover, two cross-peaks, one above and the other below the diagonal are expected between the two states, as they arise from the correlation between two transitions in the same molecule[24]. The lower cross-peak between the two states is weak, but clearly visible. However, the cross-peak above the diagonal is not visible, because of its overlap with the negative Q_y excited state absorption signal.

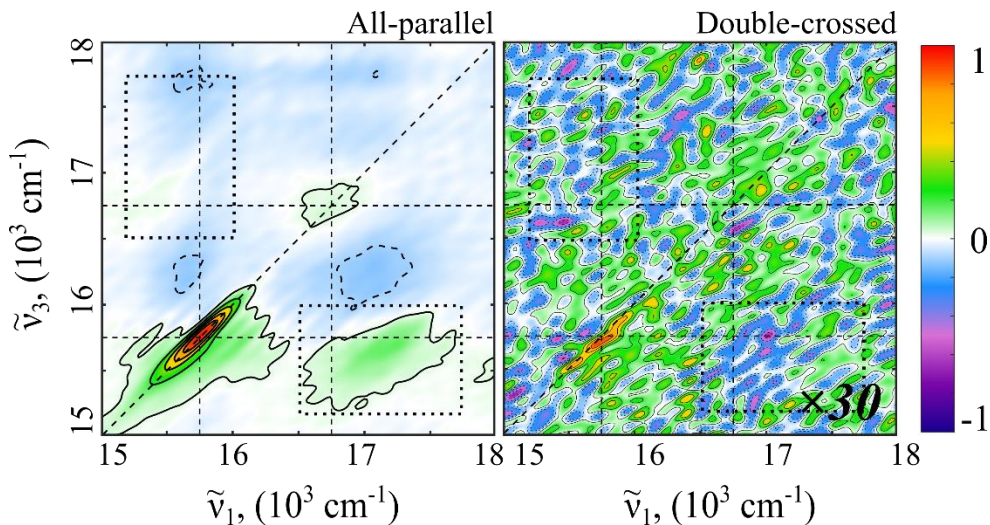


Fig. 2. 2DES spectra at the population time $t_2=100$ fs. Real (absorptive) component of the total (rephasing + non-rephasing) part of the 2DES spectra at 77 K is shown, measured with the two polarization sequences: AP (all-parallel, left) and DC (double-crossed, right). Dashed line crossings mark positions of two major transitions at 15750 cm^{-1} and 16750 cm^{-1} . Dotted rectangles mark the cross-peak areas, integrated to obtain Fourier amplitudes of the beatings. The DC spectrum is scaled by a factor of 30 to make weak features visible. Contour lines (solid for positive, dashed for negative signals) are spaced by every 20% of the maximum signal and additional contour line is drawn at the 2.5% to make weak signals more apparent.

Comparison of the AP and DC 2D spectra demonstrate a very large suppression of the signals originating from the interaction of laser fields with the transitions, which have parallel orientation of the transition dipole moments (see right spectrum in Fig. 2). For details regarding the estimation of the suppression factor, including a comparison of the isopropanol impulsive Raman mode signal at 810 cm^{-1} , resulting in the lower suppression factor bound of 660, see SI and Fig. S3. The “leakage” signal at the DC diagonal peak ($\tilde{\nu}_1, \tilde{\nu}_3=15750\text{ cm}^{-1}$) was used for the approximate phasing of the DC spectra. While the AP sequence detects all 2DES signals, the DC sequence suppresses most of the signals, including the energy transfer and Frank-Condon vibrational coherence signals[15]. Therefore, only beating signals from the superposition of states that are excited via transitions with non-parallel dipole moments remain. The strongest DC signal is expected for the 90° angle between the dipole moments of involved transitions. Dependence of the signal amplitude of different polarization sequences on the relative dipole angle between involved transitions was discussed in detail by Paleček et al. (see e.g. Fig. 3 in [21]). Generally, signals which are visible in the DC measurement include purely electronic coherences and coherences excited via vibronically coupled transitions[15]. In the next sections we present analysis of the complex beating signals from the AP and DC experiments in order to reveal vibronic coupling in the Chl *c1* molecule. It is noteworthy that a very large suppression factor, achieved in our experiments, was necessary for the analysis of the subtle signals arising from the vibronic coupling.

Coherence beatings and oscillation maps

After fitting and subtracting the multi-exponential kinetics from the population time evolution traces for both the AP and DC data sets, Fourier analysis was performed on the residuals of the complex data of the rephasing part. In this way, the spectral positions and amplitudes of different coherence oscillation modes (positive and negative) were obtained from the experimental data.

Fig. 3 shows Fourier transform (FT) amplitudes extracted from the cross-peak regions (upper cross-peak vs lower cross-peak) from the DC experiment. Here we focus on the 1200 cm^{-1} wavenumber region for the following reasons: (i) these are the largest amplitude beatings, and (ii) the corresponding beating frequency is close to the splitting between the two strongest transitions (marked as Q_y and Q_x in Fig. 1). In this wavenumber region, the relative amplitude ratio of the beatings between the AP and DC experiments has been estimated to be 11 ± 2 , (SI, Fig. S4). This ratio is approximately 60 times lower than the suppression factor of the unwanted signals in the DC experiments, which ensures credibility that the beatings come from superpositions excited via transitions with non-parallel dipole moments.

The most prominent positive and negative $\tilde{\nu}_2$ oscillation maps for the main wavenumbers, identified from the DC experiments, are presented in Fig. 3, together with their FT amplitude spectra. It is apparent that beatings with negative wavenumbers are present at the lower cross-peak, while beatings with the positive wavenumbers – at the upper cross-peak. Additional weaker positive $\tilde{\nu}_2$ oscillation maps are presented in Fig. S5. The integrated FT amplitudes over the cross-peaks, showing the complete $\tilde{\nu}_2$ range from both AP and DC data sets are summarized in Fig. S6. In addition, $\tilde{\nu}_2$ oscillation maps for the strongest beatings in the AP measurement are presented in Fig. S7.

The strongest DC coherence signals in the upper cross-peak have $+1070\text{ cm}^{-1}$ and $+1200\text{ cm}^{-1}$ wavenumbers, while the corresponding region in the lower cross-peak area is dominated by beatings of five wavenumbers: -1540 cm^{-1} , -1280 cm^{-1} , -1230 cm^{-1} , -1180 cm^{-1} and -1000 cm^{-1} . In the following section we discuss the origin of these beatings and their significance for understanding the photophysical properties of the chlorophyll-type molecules.

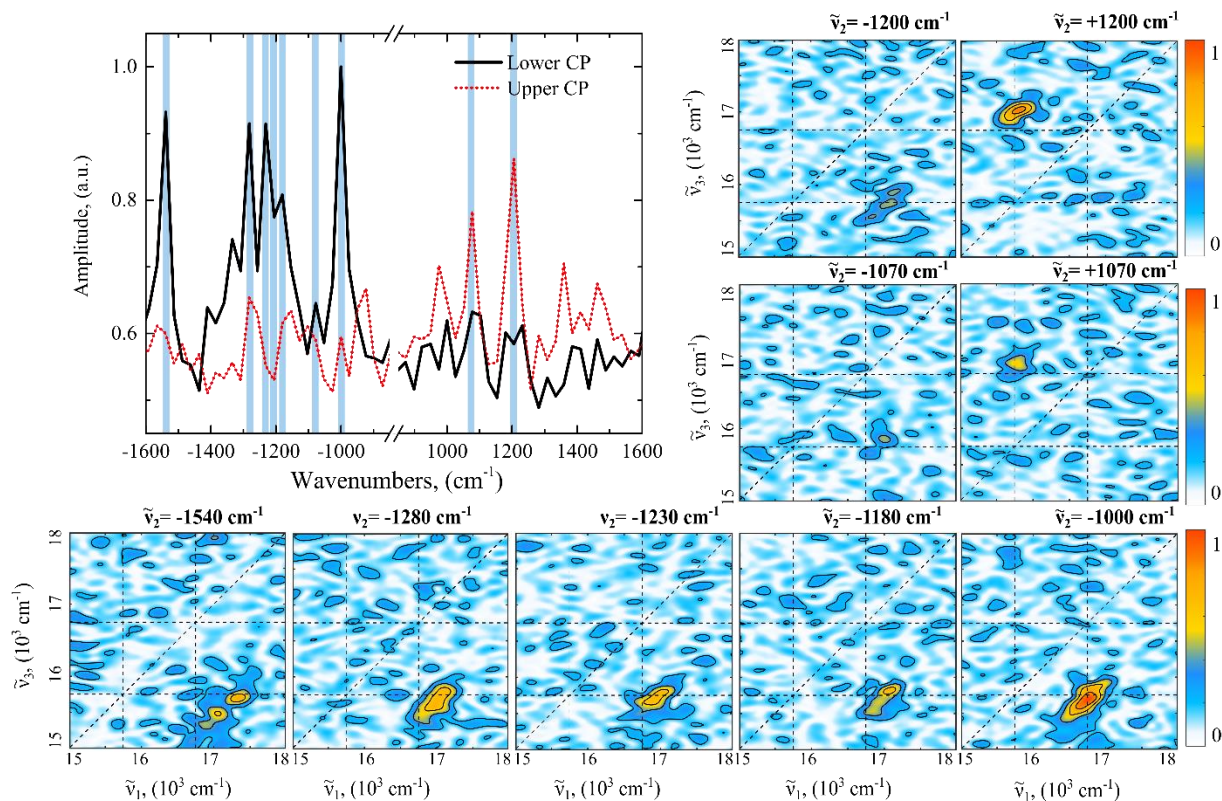


Fig. 3. Analysis of the complex beating signals from the DC data set. Fourier transform amplitude obtained from the cross-peak (CP) regions (lower vs upper), after fitting the rephasing part of the kinetics with multi-exponential decay/rise and subtracting the fits from the signal. The low wavenumber ($<800 \text{ cm}^{-1}$) region is presented in Fig. S6. For the Fourier amplitude spectra, data from both cross-peaks was normalized to the amplitude of the -1000 cm^{-1} wavenumber peak. Positive and negative $\tilde{\nu}_2$ oscillation maps of selected wavenumbers (marked with light blue bars in the amplitude graph) are also presented. The corresponding wavenumbers are (from left to right in the amplitude graph): -1540 cm^{-1} , -1280 cm^{-1} , -1230 cm^{-1} , -1200 cm^{-1} , -1180 cm^{-1} , -1070 cm^{-1} , -1000 cm^{-1} , $+1070 \text{ cm}^{-1}$, $+1200 \text{ cm}^{-1}$. Maps were normalized to the maximum intensity of the -1000 cm^{-1} beating map. Some additional lower-amplitude positive wavenumbers oscillation maps are presented in Fig. S5.

Discussion

The energy relaxation between Q states in chlorophylls is known to take place on the 100 fs timescale[26,27]. In the presented data we did not directly observe “ $Q_x \rightarrow Q_y$ ” energy relaxation in the Chl *c1* molecule, as there is neither an observable decay in the upper diagonal peak nor a rise of the lower cross-peak in the time traces after 80 fs (see Fig. S8). As mentioned above, the first 80 fs in the measurements are unreliable, because of the unavoidable presence of the multiple artefacts. Since the internal conversion has to be present, the lack of observable decay indicates that it must happen within 80 fs. Reimers et al. reported that the most important factors determining the internal relaxation are coupling strength and resonance between the unperturbed energy gap between the Q states and the vibrational frequency[3]. Our data indicates that this relaxation in Chl *c1* is extremely fast and takes place on the 50 fs time scale, pointing to a strong vibronic coupling. At the moment we are unable to provide a more quantitative estimate. This presents an

excellent opportunity for the future studies of vibronic coupling, which will have to involve rigorous modeling.

Next we discuss the origin of the quantum beats “surviving” in the DC experiment. Remarkably, coherence beatings in Chl *c1* molecules present a very rich and complex picture. As discussed in detail in the SI, the suppression factor of the signals originating from the interaction with all parallel transition dipole moments is at least 660. Therefore, all the “leakage” signals are expected to be very weak and do not need to be considered. Such signals include coherences arising from the superposition of two states having parallel transition dipole moments, such as Franck-Condon vibrational coherences in the ground or excited electronic states.

The only beating signals which could be visible in the DC experiment are either electronic coherences or coherences excited via vibronically coupled transitions[5,14,15,28]. Purely electronic coherences are not visible in our analysis primarily due to their fast dephasing times (upper limit of ~ 100 fs) due to the extremely short lifetime of the upper electronic state. The beatings observed in our measurements dephase on the time scale from hundreds of femtoseconds to more than a picosecond, see SI, Fig. S9, Table S1. Therefore, we come to a conclusion that apparent coherences in the DC experiments in the range of 1000 cm^{-1} to 1540 cm^{-1} wavenumbers are coherences excited via vibronically coupled transitions, thus providing direct evidence for the presence of vibronic coupling between the Q_x and Q_y states, as suggested by Reimers and co-authors[3]. They used a vibronic coupling model to successfully fit the absorption and magnetic circular dichroism spectra of a series of chlorophyll-type molecules. As expected, the strongest vibronic mixing occurred close to the resonance condition – when the *unperturbed* energy gap between the uncoupled Q_y and Q_x transitions is close to an *unperturbed* vibrational mode of the molecule. State mixing results in changes of transition dipole moment orientations, and in turn allows for excitation of both ground and excited state vibrational coherences via transitions with non-parallel dipole moments[5,14,15], which we observe in the DC experiments.

In agreement with Reimers et al.[3] we propose that the two lowest energy states visible in the low temperature absorption spectrum (at 15670 cm^{-1} and 16870 cm^{-1} in Fig. 1), correspond to the Q_y state (with very small contribution of the Q_x character) and vibronically mixed Q_x state (with a substantial Q_y character), respectively. Since the third transition at 17850 cm^{-1} is not observed in the 2DES experiments, we did not obtain the information regarding its origin. However, it is reasonable to speculate that it is the higher-energy state resulting from vibronic mixing of the Q_y and Q_x states.

Now we consider the wavenumbers and relative amplitudes of the observed vibronic beatings. As discussed by Butkus et al.[24], presence of the *positive* wavenumber signals above the diagonal in the rephasing part of the signal indicates presence of excited state coherences. Since we clearly see such beatings, they must originate from the vibrational coherences in the electronically excited states. Note that we observe at least two well-resolved wavenumbers 1070 cm^{-1} and 1200 cm^{-1} . This means that there is more than one vibrational mode leading to the vibronic coupling between the Q_y and Q_x states. Detection of additional wavenumbers in quantum beats means additional transitions, which are not, however, observed in the absorption spectrum (Fig. 1). This is most likely due to the inhomogeneous broadening effect. It has been shown that inhomogeneous

broadening does not affect vibrational coherences as strongly as absorption lineshape or electronic coherences[29]. Nonetheless, since we are dealing with a vibronic case, further investigation is required to determine to what extent insensitivity to inhomogeneous broadening holds for the coherences observed in our experiments.

Presence of the *negative* wavenumbers below the diagonal could indicate both excited and ground state coherences[24]. The excited state coherences lead to the beating signals with equal amplitudes at positive/negative wavenumbers located in the cross-peak positions above/below the diagonal. Such symmetry is clearly absent in our data, as the negative -1070 cm^{-1} and -1200 cm^{-1} wavenumber beatings below the diagonal are much weaker than the corresponding positive counterparts. Instead, the below diagonal cross-peak area is dominated by several other wavenumbers: -1540 cm^{-1} , -1280 cm^{-1} , -1230 cm^{-1} , -1180 cm^{-1} and -1000 cm^{-1} , which are not present above diagonal (with exception of the $+1000\text{ cm}^{-1}$ wavenumber). One conclusion that we make is that the signals below the diagonal are dominated by vibrational coherences in the ground electronic state, excited by the impulsive Raman process[5]. It is more difficult to explain the observation of at least five wavenumbers. One possible interpretation is that we see several vibrational modes, which are not involved in the vibronic coupling between the Q_y and Q_x states, but have appreciable Huang-Rhys factor. Such coherences can in principle be observed in the DC experiments, because they can be excited via vibronically mixed transitions. The observed wavenumbers approximately match the Chl *c* Raman signals present in the $1000\text{--}1500\text{ cm}^{-1}$ region[30]. It is also important to note here that the differences between the oscillation wavenumbers of the observed beating wavenumbers are not too far from the experimental resolution (25 cm^{-1}). Therefore, there is some uncertainty if all of the wavenumbers represent different superpositions, and thus different vibrational modes, or if some of them come from limitations of the analysis.

The important question to address is if vibronic coupling observed in Chl *cI* is a general feature of all chlorophyll-type molecules. First thing to note is that the electronic structure persists throughout the chlorophyllide family, featuring two main electronic transitions – Q_y and Q_x [3,12], despite some variation of macrocycle structure (e.g. porphyrins (Chls *c*) vs chlorins (Chls *a/b/d/f*)). On the other hand, the different side chains as well as small changes in the pyrrole rings alters some vibrational frequencies of these molecules (see e.g. [31] and references therein). However, it is reasonable to assume that the presence of a broad range of vibrations at different wavenumbers and of various type enables vibronic coupling in each chlorophyll-type molecule. An important direction for the future studies will be to explore which frequency vibrations are responsible for the vibronic coupling and if they correspond to similar molecular motions in different chlorophyll-type molecules. Highly successful application of the vibronic coupling model by Reimers and co-workers[3] lends a very strong support that vibronic coupling is indeed present in all of the members of the chlorophyllide family.

This leads to proposition that vibronic coupling between the Q_y and Q_x states should be taken into account when studying photophysical properties of chlorophyll-type molecules and their multiple functions in biological systems. It is currently debated if vibronic coupling in molecular dimers and oligomers is important for light harvesting and primary charge separation functions in

photosynthetic systems[5,32] . Vibronically mediated transfers are suggested to enhance the rates of electronic relaxations[4], in addition, vibronic coupling may speed up the charge separation process in reaction centers[33,34]. This phenomenon was also suggested to explain the ultrafast carotenoid to chlorophyll energy transfer in the LH2 complex[35]. Better understanding of vibronic coupling, both qualitative and quantitative is very challenging, nevertheless it might prove necessary for explaining efficient and robust primary photosynthetic phenomena.

Conclusions

While the role of the vibronic coupling in photosynthetic functions remains to be clarified, with the help of polarization-controlled 2DES we directly unveiled vibronic coupling between two electronic states of the photosynthetic pigment Chl *c1*. This coupling appears to be realized via at least two vibrational modes. It is also clear that inhomogeneous broadening in the linear spectra hides the features arising from the complexity of the vibronic coupling, which is nevertheless revealed in the study of coherent beats. This coupling is expected to be present in all chlorophyll-type molecules, and therefore should be taken into account when modelling their photophysical properties and their function as light-harvesting and charge-separation co-factors in photosynthetic complexes.

Competing interests: none.

Acknowledgements

Work in Lund was supported by the Swedish Research Council. CB and AH acknowledge support from the Deutsche Forschungsgemeinschaft [grant number DFG Bu 812/10-1] and from the European Union's Horizon2020 research and innovation programme under the Marie Skłodowska-Curie grant agreement No 675006 (SE2B).

References

- [1] R.E. Blankenship, *Molecular Mechanisms of Photosynthesis*, Blackwell Science, 2002. doi:10.1002/9780470758472.
- [2] M. Gouterman, Spectra of porphyrins, *J. Mol. Spectrosc.* 6 (1961) 138–163. doi:10.1016/0022-2852(61)90236-3.
- [3] J.R. Reimers, Z.L. Cai, R. Kobayashi, M. Rätsep, A. Freiberg, E. Krausz, Assignment of the Q-Bands of the Chlorophylls: Coherence Loss via Qx-Qy Mixing, *Sci. Rep.* 3 (2013) 2761. doi:10.1038/srep02761.
- [4] J.M. Womick, A.M. Moran, Vibronic enhancement of exciton sizes and energy transport in photosynthetic complexes, *J. Phys. Chem. B.* 115 (2011) 1347–1356. doi:10.1021/jp106713q.
- [5] V. Tiwari, W.K. Peters, D.M. Jonas, Electronic resonance with anticorrelated pigment vibrations drives photosynthetic energy transfer outside the adiabatic framework, *Proc. Natl. Acad. Sci. U. S. A.* 110 (2013) 1203–1208. doi:10.1073/pnas.1211157110.
- [6] D.M. Jonas, Two-Dimensional Femtosecond Spectroscopy, *Annu. Rev. Phys. Chem.* 54 (2003) 425–463. doi:10.1146/annurev.physchem.54.011002.103907.

- [7] T. Brixner, J. Stenger, H.M. Vaswani, M. Cho, R.E. Blankenship, G.R. Fleming, Two-dimensional spectroscopy of electronic couplings in photosynthesis, *Nature*. 434 (2005) 625–628. doi:10.1038/nature03429.
- [8] E. Meneghin, C. Leonardo, A. Volpato, L. Bolzonello, E. Collini, Mechanistic insight into internal conversion process within Q-bands of chlorophyll a, *Sci. Rep.* 7 (2017) 11389. doi:10.1038/s41598-017-11621-2.
- [9] S.S. Senlik, V.R. Policht, J.P. Ogilvie, Two-Color Nonlinear Spectroscopy for the Rapid Acquisition of Coherent Dynamics, *J. Phys. Chem. Lett.* 6 (2015) 2413–2420. doi:10.1021/acs.jpcclett.5b00861.
- [10] V.R. Policht, A. Niedringhaus, J.P. Ogilvie, Characterization of Vibrational Coherence in Monomeric Bacteriochlorophyll a by Two-Dimensional Electronic Spectroscopy, *J. Phys. Chem. Lett.* 9 (2018) 6631–6637. doi:10.1021/acs.jpcclett.8b02691.
- [11] E. Songaila, R. Augulis, A. Gelzinis, V. Butkus, A. Gall, C. Büchel, B. Robert, D. Zigmantas, D. Abramavicius, L. Valkunas, Ultrafast energy transfer from chlorophyll c 2 to chlorophyll a in fucoxanthin-chlorophyll protein complex, *J. Phys. Chem. Lett.* 4 (2013) 3590–3595. doi:10.1021/jz401919k.
- [12] M. Helfrich, B. Bommer, U. Oster, H. Klement, K. Mayer, A.W.D. Larkum, W. Rüdiger, Chlorophylls of the c family: Absolute configuration and inhibition of NADPH:protochlorophyllide oxidoreductase, *Biochim. Biophys. Acta - Bioenerg.* 1605 (2003) 97–103. doi:10.1016/S0005-2728(03)00081-1.
- [13] V.P. Singh, M. Westberg, C. Wang, P.D. Dahlberg, T. Gellen, A.T. Gardiner, R.J. Cogdell, G.S. Engel, Towards quantification of vibronic coupling in photosynthetic antenna complexes, *J. Chem. Phys.* 142 (2015) 212446. doi:10.1063/1.4921324.
- [14] E. Thyrgaug, R. Tempelaar, M.J.P. Alcocer, K. Židek, D. Bina, J. Knoester, T.L.C. Jansen, D. Zigmantas, Identification and characterization of diverse coherences in the Fenna-Matthews-Olson complex, *Nat. Chem.* 10 (2018) 780–786. doi:10.1038/s41557-018-0060-5.
- [15] D. Paleček, P. Edlund, S. Westenhoff, D. Zigmantas, Quantum coherence as a witness of vibronically hot energy transfer in bacterial reaction center, *Sci. Adv.* 3 (2017) 9. doi:10.1126/sciadv.1603141.
- [16] L. Provasoli, J.J.A. McLaughlin, M.R. Droop, The development of artificial media for marine algae, *Arch. Mikrobiol.* 25 (1957) 392–428. doi:10.1007/BF00446694.
- [17] S.W. Jeffrey, G.F. Humphrey, New spectrophotometric equations for determining chlorophylls a, b, c1 and c2 in higher plants, algae and natural phytoplankton. *Biochemical Physiology Pflanz* 167: 191–194., *Biochem. Physiol. Pflanz.* 167 (1975) 191–194. doi:10.1016/0022-2860(75)85046-0.
- [18] S.W. Jeffrey, R.F.C. Mantoura, T. Bjørnland, Data for the identification of 47 key phytoplankton pigments. In: S.W. Jeffrey, R.F.C. Mantoura und S.W. Wright (Hg.): *Phytoplankton pigments in oceanography: guidelines to modern methods*. Paris: UNESCO Pub. (1997) 449–559

- [19] R. Augulis, D. Zigmantas, Detector and dispersive delay calibration issues in broadband 2D electronic spectroscopy, *J. Opt. Soc. Am. B.* 30 (2013) 1770–1774. doi:10.1364/josab.30.001770.
- [20] R. Augulis, D. Zigmantas, Two-dimensional electronic spectroscopy with double modulation lock-in detection: enhancement of sensitivity and noise resistance, *Opt. Express.* 19 (2011) 13126–13133. doi:10.1364/OE.19.013126.
- [21] D. Paleček, P. Edlund, E. Gustavsson, S. Westenhoff, D. Zigmantas, Potential pitfalls of the early-time dynamics in two-dimensional electronic spectroscopy, *J. Chem. Phys.* 151 (2019) 024201. doi:10.1063/1.5079817.
- [22] H. Li, A.D. Bristow, M.E. Siemens, G. Moody, S.T. Cundiff, Unraveling quantum pathways using optical 3D Fourier-transform spectroscopy, *Nat. Commun.* 4 (2013) 1390. doi:10.1038/ncomms2405.
- [23] J. Seibt, T. Hansen, T. Pullerits, 3D spectroscopy of vibrational coherences in quantum dots: Theory, *J. Phys. Chem. B.* 117 (2013) 11124–11133. doi:10.1021/jp4011444.
- [24] V. Butkus, J. Alster, E. Bašinskaite, R. Augulis, P. Neuhaus, L. Valkunas, H.L. Anderson, D. Abramavicius, D. Zigmantas, Discrimination of Diverse Coherences Allows Identification of Electronic Transitions of a Molecular Nanoring, *J. Phys. Chem. Lett.* 8 (2017) 2344–2349. doi:10.1021/acs.jpcllett.7b00612.
- [25] S.W. Jeffrey, S.W. Wright, A new spectrally distinct component in preparations of chlorophyll c from the micro-alga *Emiliana huxleyi* (Prymnesiophyceae), *BBA - Bioenerg.* 894 (1987) 180–188. doi:10.1016/0005-2728(87)90188-5.
- [26] Y. Shi, J.Y. Liu, K.L. Han, Investigation of the internal conversion time of the chlorophyll a from S3, S2 to S1, *Chem. Phys. Lett.* 410 (2005) 260–263. doi:10.1016/j.cplett.2005.05.017.
- [27] H.M. Visser, O.J. Somsen, F. van Mourik, S. Lin, I.H. van Stokkum, R. van Grondelle, Direct observation of sub-picosecond equilibration of excitation energy in the light-harvesting antenna of *Rhodospirillum rubrum*, *Biophys. J.* 69 (1995) 1083–1099. doi:10.1016/S0006-3495(95)79982-9.
- [28] S. Westenhoff, D. Paleček, P. Edlund, P. Smith, D. Zigmantas, Coherent picosecond exciton dynamics in a photosynthetic reaction center, *J. Am. Chem. Soc.* 134 (2012) 16484–16487. doi:10.1021/ja3065478.
- [29] V. Butkus, D. Zigmantas, D. Abramavicius, L. Valkunas, Distinctive character of electronic and vibrational coherences in disordered molecular aggregates, *Chem. Phys. Lett.* 587 (2013) 93–98. doi:10.1016/j.cplett.2013.09.043.
- [30] N. Parab, V. Tomar, Raman spectroscopy of algae: A review, *J. Nanomedicine Nanotechnol.* 3 (2012) 1000131. doi:10.4172/2157-7439.1000131.
- [31] J. Du, T. Teramoto, K. Nakata, E. Tokunaga, T. Kobayashi, Real-time vibrational dynamics in chlorophyll a studied with a few-cycle pulse laser., *Biophys. J.* 101 (2011) 995–1003. doi:10.1016/j.bpj.2011.07.011.

- [32] Y. Fujihashi, M. Higashi, A. Ishizaki, Intramolecular Vibrations Complement the Robustness of Primary Charge Separation in a Dimer Model of the Photosystem II Reaction Center, *J. Phys. Chem. Lett.* 9 (2018) 4921–4929. doi:10.1021/acs.jpcllett.8b02119.
- [33] F.D. Fuller, J. Pan, A. Gelzinis, V. Butkus, S.S. Senlik, D.E. Wilcox, C.F. Yocum, L. Valkunas, D. Abramavicius, J.P. Ogilvie, Vibronic coherence in oxygenic photosynthesis, *Nat. Chem.* 6 (2014) 706–711. doi:10.1038/nchem.2005.
- [34] E. Romero, R. Augulis, V.I. Novoderezhkin, M. Ferretti, J. Thieme, D. Zigmantas, R. Van Grondelle, Quantum coherence in photosynthesis for efficient solar-energy conversion, *Nat. Phys.* 10 (2014) 676–682. doi:10.1038/NPHYS3017.
- [35] E. Thyryhaug, C.N. Lincoln, F. Branchi, G. Cerullo, V. Perlík, F. Šanda, H. Lokstein, J. Hauer, Carotenoid-to-bacteriochlorophyll energy transfer through vibronic coupling in LH2 from *Phaeosprillum molischianum*, *Photosynth. Res.* 135 (2018) 45–54. doi:10.1007/s11120-017-0398-3.